Comparing Telescope Performance of Overlapping Wavelength Ranges for Exoplanet Direct Imaging

Avital Keeley*
Department of Physics, University of California Santa Barbara (2022 Physics REU)
Department of Physics and Astronomy, Eastern Michigan University

Dr. Maxwell Millar-Blanchaer (Faculty Advisor)†
Department of Physics, University of California Santa Barbara

Skyler Palatnick (Graduate Student Mentor)
Department of Physics, University of California Santa Barbara
(Dated: September 23, 2022)

Predicted planet-mass sensitivities were calculated for a list of instruments based on their contrast curves and evolutionary models. These masses were compared for star systems specified by the stellar apparent magnitude, distance, and age of the target star. The resultant plots allow easy direct comparison of instrument performance. The plots provide information on the calculated masses, optimal imaging separations, and the accuracy of the planet to that simulated by evolutionary models.

I. INTRODUCTION

Since the first exoplanet was confirmed in 1992, direct imaging (DI) has become a vital method for detecting, confirming, and characterizing exoplanets. By imaging the planet itself, DI is able to measure key features including the planet's mass, radius, orbital period, gravity, and atmosphere. These data describe planet formation which, in turn, improves hypotheses of solar system formations. DI is most efficient when imaging younger planets and/or planets farther from their stars. Younger planets have higher temperatures which corresponds to larger contrasts. Contrast refers to the ratio of planet light to star light. Logically, then, DI strives to optimize the contrast to produce the highest resolution image of a planet.

In Fig. 1, from Skemer et. al, the contrast of multiple planets at various temperatures is plotted as a function of the wavelengths at which they can be imaged [1]. In addition to the wavelength values, the x axis also denotes the pass bands associated with them. This plot can also be used to track a single planet as it cools, so it can always be imaged in the most optimal pass band. These bands encompass wavelength ranges commonly imaged, which exclude wavelengths at which chemical phenomena (such as the emission line of oxygen) appear to produce the highest resolution image [2].

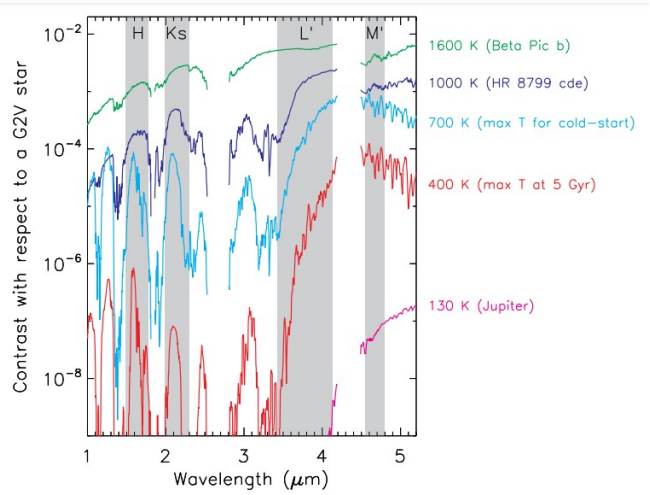

FIG. 1. Contrast as a function of the wavelength at which planets are imaged. This plot shows the change in contrast with respect to temperature [1].

Current DI instruments can sufficiently image to 10^{-6}, but future instrumentation aims to detect planets at contrasts around 10^{-9}. Additionally, the next generation of DI technology will improve the separation at which they can image to < 0.2" [3].

The performance of each instruments' measuring contrast and separation is plotted as a contrast curve which plots the contrast an instrument can image as a function of the separation between the planet and host star. Fig. 2 shows the contrast curve for CHARIS under good conditions that was digitized for use in the code.

* avital.keeley@gmail.com
† http://web.physics.ucsb.edu/~maxmb/index.html

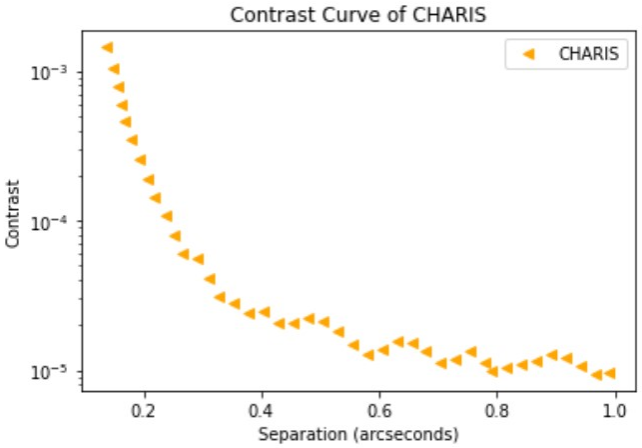

FIG. 2. A contrast curve of CHARIS which plots contrast vs. separation. These data were digitized from a run with good conditions [4].

With contrast curves, the capabilities of different instruments can be compared. The most important data in comparing contrast curves, though, is the wavelength at which the instrument images. This is also where DI has reduced its efficiency. When two instruments can image in the same wavelengths at similar contrast values, it is unclear which instrument will produce the highest resolution image of the target system. For example, CHARIS images 1150 to 2390 micrometers [5]. NIRC2, however, can also image that range and more [6]. Fig. 3 shows the contrast curves of these two instruments in a single plot.

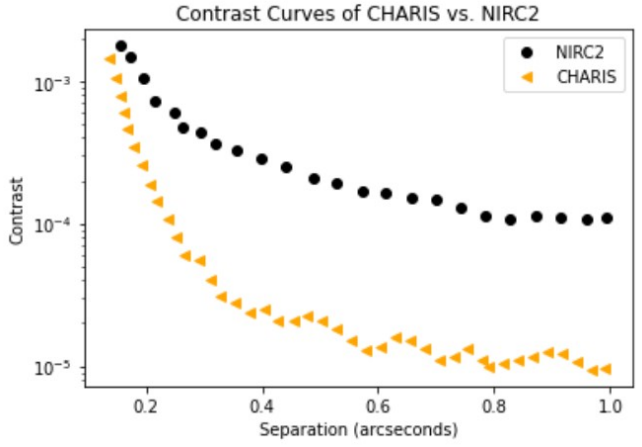

FIG. 3. Contrast curves of CHARIS and NIRC2 plotted on a single plot to directly compare their capabilities.

In this case, any planet at a contrast and separation above the contrast curves could be imaged by both instruments. This overlap creates the possibility of imaging the target with a sub-optimal instrument, which would unnecessarily hinder the target's characterization (e.g. produce a range of predicted mass that is lower than would be calculated if the planet was characterized with the optimal instrument). By using an inferior instrument, the images may create characterizations of a planet's chemistry, gravity, atmosphere, and mass at a lower resolution and worse quality than if they had been obtained with the ideal instrument. The most suitable instrument would image the planets at the highest contrast possible, which depends on parameters of the stellar system as well as the capabilities of the instrument. Therefore, we created a program to compare instruments' sensitivity to exoplanet masses. This program determines the most suitable instrument for a specified star system, increasing the efficiency of the telescope time and related resources.

II. INPUTS AND OUTPUTS

To calculate the masses to which each instrument is sensitive, the code takes characteristics of the target system as inputs to interpolate between model data. That is, the code includes data from each instrument uploaded (which is also the list of instruments available to select for the code) and multiple evolutionary models. At the time this paper is written, the instruments include CHARIS and GPI 1.0. The contrast curves of each instrument available are digitized, and their respective contrast and separation data is uploaded into the code. The evolutionary models available for interpolation include COND, Dusty, BT Settl, and BEX.

The importance of incorporating multiple models arises from the assumptions of the planet's features that are implemented by respective models (e. g. DUSTY accounts for dust in the planet's atmosphere). By including more models that encompass a larger variety of planet types, the program can calculate planet masses with more accuracy. And, additionally, including a larger diversity of models allows for imaging more expansive types of planets. The models, then, provide accuracy to the calculated masses and allow the program to widen the range of planets imaged.

Along with the foundational data, the code requires the user to specify the characteristics of the target star: the apparent stellar magnitude, the age of the system in gigayears (Gyr), and the distance to the system in parsecs (pc). With these three parameters and the model data, the code can interpolate the mass of a planet using a function created by Vanessa Bailey (contrast_utils.py). A mass for an expected planet is calculated for each magnitude value. This list of masses is calculated for each instrument specified by the user in a second function which compares instrument capabilities. Finally, the contrast curves of each instrument are plotted against each other and a second plot displays the mass vs. separation data of each instrument.

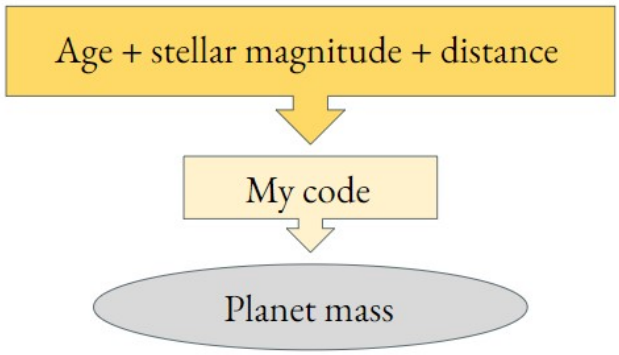

FIG. 4. Flowchart of the code's inputs and outputs.

Fig. 4 shows the main components of the code and their place in the overall structure. The three main inputs are specified by the user to define the target system. However, this diagram relays only a simplified process of the code that accepts the target system parameters and calculates exoplanet masses. The most important element in the code is the collection of various evolutionary models. Data from these models are included in the database, the beginning of the code that contains information and data from the instruments and evolutionary models available for selection; and it is these models that connect the input parameters listed in Fig. 4 to predicted planet masses. Thereby, Fig. 4 can be expanded one step out to showcase this as is evident in Fig. 5.

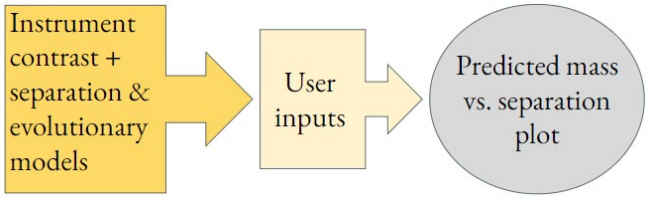

FIG. 5. A more detailed flowchart of Fig. 4 including the database containing the evolutionary models.

This figure shows that the database lays the foundation of the code that allows the proceeding steps. The user inputs are actually a secondary input that connect the math in the models to real data, enabling the code to calculate quantitative masses for the specified system.

III. METHODS

A. Computation

To obtain the contrast and separation data of each instrument in the code, plots of their contrast curves had to be digitized into a .txt file. The Web Plot Digitizer website (`https://apps.automeris.io/wpd/`) allows a user to import an image and select the data to be converted to a table. These tables were then imported into the code to comprise the database of instruments that can be used.

Also included in the initial database are lists including data from various evolutionary models. These include the age, mass, and magnitudes of the simulated planet. It is these data that are used as the base for the interpolation functions. Using the evolutionary models, the interp1d functions in the code (imported from scipy) interpolate to the user inputs (stellar magnitude, age, distance).

In order for the function to call the correct pass band in the evolutionary model, the code required a connection between the selected instrument and its pass band to the pass bands in each evolutionary model. To accomplish this, the code includes two dictionaries: the first of these includes the names of each instrument available as keys. Their values were written as dictionaries of each instruments' respective pass band(s). The second dictionary establishing this connection simply lists the pass bands used in the model and the names of the columns in which that data is found. This connection is completed by calling the band in the function by specifying it through the selected instrument.

B. Instruments and Evolutionary Models

The goal for the database of instruments and evolutionary models is to maximize the applicability of the code. Logically, then, the instruments and models selected for use in the code should represent the widest variety in every parameter relevant to these components: types of planet formation, the age of the system, the number of pass bands available, the range of imageable separations, the range of contrasts, and the magnitudes at which these instruments take images.

Currently, the database contains only two instruments: CHARIS and GPI. These instruments are well suited for comparison based on their pass bands. That is, since CHARIS can image in the J, H, or K band, and GPI images the Y, J, H, K1, and K2 bands, there is a lot of overlap in the stars that both instruments are capable of imaging [5] [7]. Thus, these instruments sometimes require further examination of their capabilities to determine which one would produce better images of a target. The difference in their performances emerges from the magnitude of the star. Fig. 6 highlights the differences in instrument performance on stars of different magnitudes.

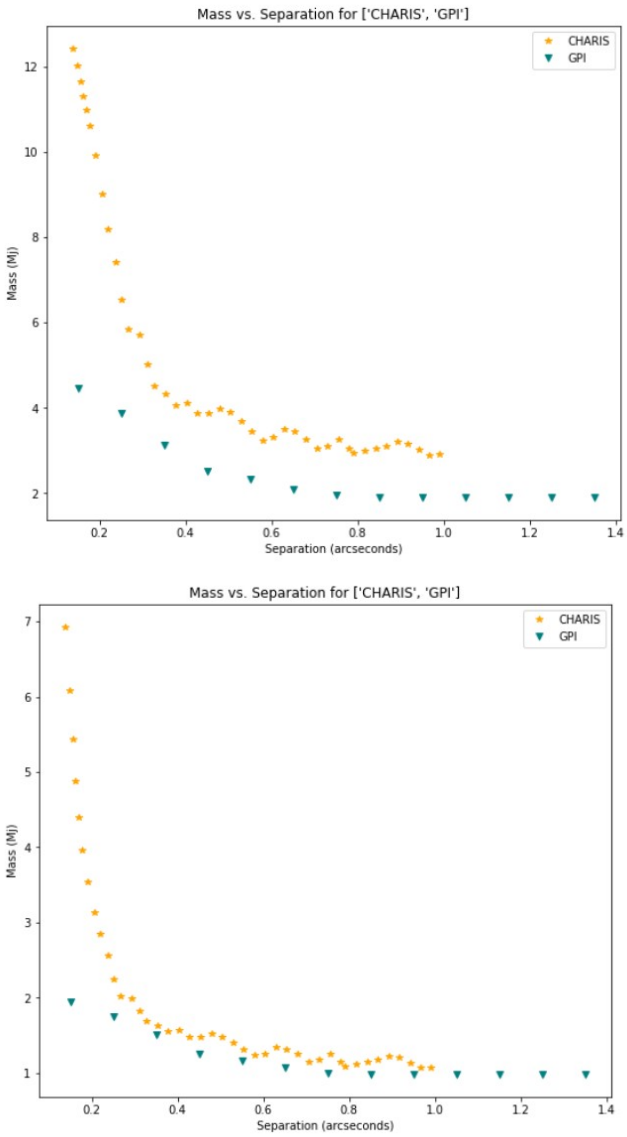

FIG. 6. A plot displaying the predicted mass as a function of separation for CHARIS and GPI. This run assumed a system age of 0.084 Gyrs, a distance of 91 pc, and used the Dusty evolutionary model. The top plot assumes a stellar of magnitude of 6 versus the bottom plot's magnitude of 9.

This figure demonstrates well the effect of stellar magnitude on resultant mass predictions. At a stellar magnitude of 6, there is a large enough gap in the plot that, while this run was helpful to see the results directly compared, this is virtually unnecessary to rank CHARIS and GPI's capabilities. However, as the stellar magnitude increases to 9, Fig. 6 demonstrates the ambiguity that can occur between instruments' contrast capabilities. In the bottom plot of Fig. 6, the resultant masses are much more comparable between the two instruments. This comparability yields a lack of clarity in which instrument has better sensitivity at the specific parameters of the system and separation, which necessitates the code to make an educated decision.

Instruments are chosen for the code primarily for their popularity in use. That is, the code includes instruments that will be used in real observations. The code, then, includes instruments representative of the current imaging community that also demonstrate a necessity for a direct comparison of their similar capabilities.

In conjunction, the evolutionary models were chosen from their relevance to the instruments available. The most notable example of this is the inclusion of the BEX models in tandem with adding the James Webb Space Telescope (JWST) pass band list (contrast and separation data is not yet available which prevents JWST from being added completely to the database). The evolutionary models are imperative to calculating the predicted masses since they create the functions that the target system parameters are interpolated from to yield the mass. Thus, the evolutionary models encompass a wide variety of types of planets/planet formation to maximize the accuracy of results.

Including a variety of evolutionary models is vital to the accuracy of the mass predictions because the starting conditions of planet formation ultimately affect the accumulation of the planet's mass. This is evident in comparisons of masses in different models.

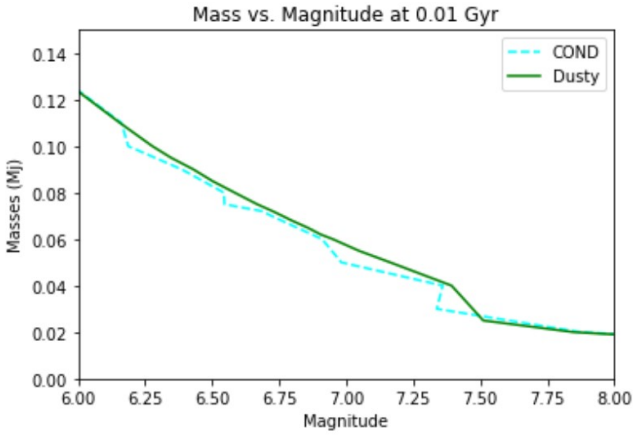

FIG. 7. A plot of masses as a function of magnitude taken from COND and Dusty models. All data is from 0.01 Gyr.

In Fig. 7, masses are plotted as a function of magnitude using data from the COND and Dusty models. The data assumes a planet age of 0.01 Gyr, which allows time for mass accumulation. This elapsed time better shows the difference in mass between the two simulated starts. Fig. 7 highlights the small discrepancies in mass between the two models which requires the inclusion of both models in the database of the code. This exemplifies the need for a range of evolutionary models with varying conditions to ensure the most accurate resultant mass values.

IV. RESULTS

With an appropriate evolutionary model selected and instruments with comparable capabilities, the code's instrument picker function ultimately yields predicted mass values associated with each instrument listed in the run. These mass values showcase the performance abilities of the respective instruments and allow the user to directly compare results to select an instrument to image the target system.

In accomplishing this, the code produces a list of planet magnitudes corresponding to the contrast values associated with the selected instrument, and it repeats this for every instrument listed in the run.

Secondly, to display the predicted mass values, the code creates a plot that shows the masses as a function of their separation from their host star for each instrument used.

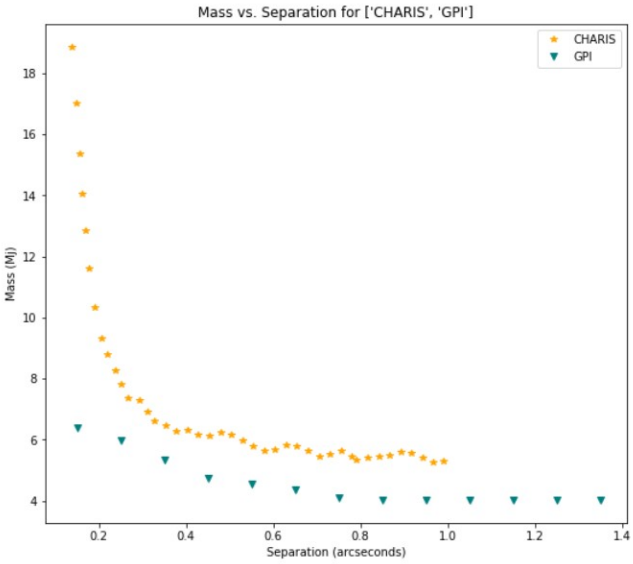

FIG. 8. An example plot of predicted masses vs. separation for CHARIS and GPI. This run assumed a stellar magnitude of 3, an age of 0.008 Gyr, and a distance of 67 pc.

This plot allows direct and easy comparison of the masses to which a selected instrument is sensitive to, and this calculation informs the decision on which instrument is most suitable for a specified system.

Lastly, alongside the mass vs. separation plot, the code creates a plot of the contrast curves of all instruments passed to the function. This reassembles the contrast and separation data taken from the individual instruments' contrast curves and plots them in a single graph.

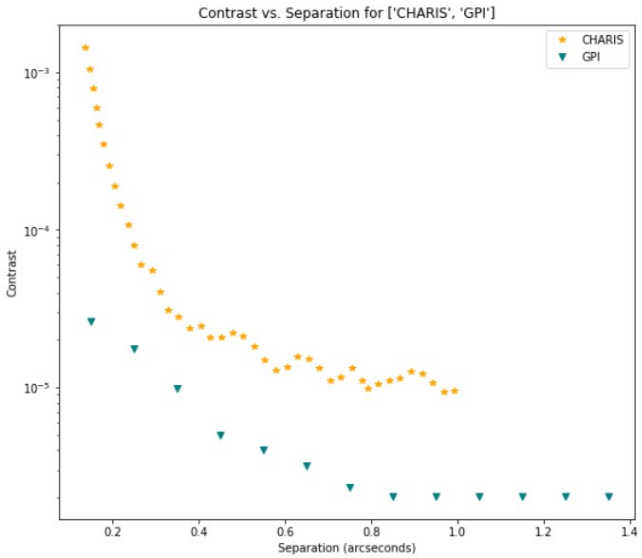

FIG. 9. Contrast curves of the listed instruments from an example run (CHARIS and GPI).

By plotting each contrast curve together, the user can also compare the general contrast curves of the instruments in addition to the predicted masses at specific parameters. These data add details to the clarification of instrument sensitivity. With the complete contrast curves, the user can compare and quantify the intersections of instruments' capabilities which informs when a given instrument is longer the optimal choice for a particular star.

V. FUTURE WORK

While this tool decisively compares performance of instruments digitized in the database, there are still many improvements to be made. Primarily, this tool can virtually always be expanded to include more instruments and models. Planned projects for space exploration in the next decade (e.g. GPI 2.0, Ronan, JWST) will provide an ample number of instruments to be added to the database as they come online for imaging. As more instruments and evolutionary models are added to the database, the code's applicability increases to include the wide range of types of exoplanets imageable.

And, in addition to the increasing applicability, there also remains work to improve the code's accuracy. For example, the code itself can still be modulized more. This will maximize its simplicity for future researchers to modify the database. Further, the representative data from each instrument can be changed to include multiple runs. This is evident in the current code with the CHARIS data which is from a run under "good conditions" [4]. Results using CHARIS, though, would be more accurate to a target system if they reflected the conditions present at the time of imaging. By adding this subcategory to the in-

strument selection, the resultant masses would be more accurate to the instrument and current conditions.

Overall, the code holds a lot of potential for improvement. While, presently, it performs its objectives and works well for its limited selection of instruments and evolutionary models, the code can only be improved by increasing the range of exoplanets to which it is applicable and adding details to the database to maximize the accuracy of the predicted values.

VI. CONCLUSION

This code successfully compares instrument capabilities and predicts exoplanet masses to which a selected instrument is sensitive to image. To do so, the code requires data about the instrument and an applicable evolutionary model, which are all included in the database section of the code. Most importantly, the code's accuracy and applicability expands with every addition to this database. While the current database options (both instruments and evolutionary models) are still severely limited, the code's modularity ensures that new instruments and models can be added easily. The instruments currently available to call in the code produce the expected results, which promises the potential for this code to become a reliable, widely used tool to optimize the direct imaging process.

ACKNOWLEDGMENTS

First, I must thank my advisor and primary investigator Dr. Max Millar-Blanchaer for his instruction and advice, and, of course, the opportunity itself to work on his team. I also want to extend my greatest gratitude to my graduate mentor, Skyler Palatnick, for his constant support and teaching. A special thanks goes to Sofia Hillman for her on-sky data analysis code and her support. Additionally, I want to thank each and every member of the Millar-Blanchaer exoplanet team for their individual support and encouragement throughout this program. This work would not have been possible without the support of Dr. Sathya Guruswamy. And, finally, I must acknowledge and thank the National Science Foundation for funding this program and my internship with grant PHY-1852574.

Appendix A: Appendix

The code in its most recently updated version can be found at this GitHub link.

[1] A. J. Skemer, M. S. Marley, P. M. Hinz, K. M. Morzinski, M. F. Skrutskie, J. M. Leisenring, L. M. Close, D. Saumon, V. P. Bailey, R. Briguglio, *et al.*, Directly imaged lt transition exoplanets in the mid-infrared, The Astrophysical Journal **792**, 17 (2014).

[2] `https://www.chroma.com/products/single-bandpass-and-single-edge-filters/application/astronomy` (2020).

[3] T. Currie, B. Biller, A.-M. Lagrange, C. Marois, O. Guyon, E. Nielsen, M. Bonnefoy, and R. De Rosa, Direct imaging and spectroscopy of extrasolar planets, arXiv preprint arXiv:2205.05696 (2022).

[4] T. Currie, O. Guyon, J. Lozi, A. Sahoo, S. Vievard, V. Deo, J. Chilcote, T. Groff, T. D. Brandt, K. Lawson, *et al.*, On-sky performance and recent results from the subaru coronagraphic extreme adaptive optics system, *Adaptive Optics Systems VII*, **11448**, 1468 (2020).

[5] `https://www.naoj.org/Projects/SCEXAO/scexaoWEB/030openuse.web/030charis.web/indexm.html` (2021).

[6] `https://www2.keck.hawaii.edu/inst/nirc2/` (2020).

[7] (2022).